

# Elastic-Scattering Measurement of the Negative-Pion Radius

E. B. Dally,<sup>(a)</sup> J. M. Hauptman,<sup>(b)</sup> J. Kubic, D. H. Stork, and A. B. Watson  
*Physics Department, University of California, Los Angeles, California 90024*

and

Z. Guzik, T. S. Nigmanov, V. D. Riabtsov, E. N. Tsyganov, and A. S. Vodopianov  
*Joint Institute for Nuclear Research, Dubna, U.S.S.R.*

and

A. Beretvas,<sup>(c)</sup> A. Grigorian,<sup>(d)</sup> J. C. Tompkins,<sup>(e)</sup> T. E. Toohig, and A. A. Wehmann  
*Fermi National Accelerator Laboratory, Batavia, Illinois 60510*

and

J. A. Poirier, C. A. Rey,<sup>(f)</sup> and J. T. Volk<sup>(g)</sup>  
*Physics Department, University of Notre Dame, Notre Dame, Indiana 46556*

and

P. D. Rapp<sup>(h)</sup> and P. F. Shepard  
*Physics Department, University of Pittsburgh, Pittsburgh, Pennsylvania 15620*  
 (Received 21 August 1981)

A new measurement of the elastic scattering of 250-GeV/c negative pions by electrons provides form-factor results from  $0.0368 < q^2 < 0.0940$  (GeV/c)<sup>2</sup>. These measurements determine the mean square pion radius to be  $\langle r_\pi^2 \rangle = 0.439 \pm 0.030$  fm<sup>2</sup> or  $\langle r_\pi^2 \rangle^{1/2} = 0.663 \pm 0.023$  fm. Comparisons are made with previous elastic-scattering experiments as well as with results obtained from electroproduction experiments,  $e^+e^-$  annihilation experiments, and phenomenological analyses.

PACS numbers: 14.40.Aq, 13.40.Fn, 13.85.Dz

Following the pioneering work of Hofstadter,<sup>1</sup> numerous electron-proton elastic-scattering experiments have determined the proton electromagnetic radius by determining the slope of the form factor in the limit of zero momentum transfer:

$$\langle r^2 \rangle = - (6 dF/dq^2)_{q^2=0}.$$

A world average<sup>2,3</sup> gives  $r_p = 0.814 \pm 0.015$  fm. The difficulty in achieving a reliable theoretical understanding of this result has motivated a search for simpler systems to study.

It might be expected that the electromagnetic radius of the charged pion would be subject to simpler theoretical treatment. Its determination by elastic scattering is difficult because of the transitory character of the pion target material. However, accurate indirect measurements have been made. Experiments on  $e^+e^-$  annihilation determine the pion form factor in the timelike region. Extraction of the pion radius,  $r_\pi = 0.678 \pm 0.008$  fm, relies upon the well-established  $\rho$  dominance<sup>4</sup> in low-energy  $e^+e^-$  interactions, but depends for its precision upon a correct modeling of the four-pion inelastic channels.<sup>5</sup> Electro-

production experiments obtain<sup>6</sup>  $r_\pi = 0.714 \pm 0.018$  fm, but require assumptions such as the equality of the pion form factor and the isovector Dirac form factor of the nucleon to provide gauge invariance in an analytic continuation to the pion pole.

The pion radius can be determined directly by elastic scattering of negative pions from electrons in a liquid-hydrogen target. Early experiments gave somewhat differing results. The first, done at Serpukhov<sup>7</sup> (S) with pion beam energy of 50 GeV and a  $q^2$  range of 0.0135 to 0.0359 (GeV/c)<sup>2</sup>, gave  $r_\pi = 0.78 \pm 0.10$  fm. The second, done at Fermilab<sup>8</sup> (F1) with beam energy of 100 GeV and a  $q^2$  range of 0.0307 to 0.0715 (GeV/c)<sup>2</sup>, gave  $r_\pi = 0.56 \pm 0.04$  fm. We report here on a second Fermilab experiment (F2) done with beam energy of 250 GeV over a  $q^2$  range of 0.0368 to 0.0940 (GeV/c)<sup>2</sup>.

This experiment was carried out simultaneously with an experiment to determine the electromagnetic form factor of the negative kaon.<sup>9</sup> The Fermilab M1 beam line provided, at 250 GeV, a negative particle flux which averaged  $2.6 \times 10^5$  usable particles per spill and which contained

98% pions and 2% kaons. The pions and kaons were distinguished by a differential Čerenkov counter. The details of the event trigger are given in Ref. 9.

A narrow-angle magnetic spectrometer employed the high resolution and high redundancy of 32 proportional-wire-chamber planes and 32 drift-chamber planes together with lead-glass shower counters for electron identification. The experiment differed from the kaon measurement<sup>9</sup> in only two regards. The pion trigger was pre-scaled down by a factor of 4, and there was a two-particle trigger requirement formed by a scintillation counter hodoscope. Subsequently the pre-scaler has been tested under a variety of conditions and found to perform satisfactorily. The trigger efficiency ( $0.999 \pm 0.001$ ) of the hodoscope has been determined from the kaon data in which it was latched. Its geometric efficiency was typically 100%, but dropped as low as 73% near the high end of the  $q^2$  range.

Beam tracks entering the electron target and the secondary tracks leaving the target, both before and after traversing the magnet, were found and fitted by straight lines. Each event was then tested against the hypothesis of elastic scattering with an unseen photon radiated in the electron's direction. The undetected photon could be produced either by radiation accompanying the elastic scattering or by electron bremsstrahlung in the target or spectrometer material. Elastic scatters were identified by requiring (1) a scattering vertex in the target, (2) a  $\chi^2$  less than 30 for the three-constraint fit, (3) a radiated photon determined in the fit to have less than 12 GeV en-

ergy, and (4) a shower-counter pulse height consistent with the electron energy. 13945 events survived the cuts which are shown in Fig. 1.

To obtain the differential  $\pi$ - $e$  elastic-scattering cross section a series of corrections were applied. No corrections were required for misidentified event vertices [Fig. 1(a)]. The largest correction [ $(12.8 \pm 0.3)\%$  to  $(18.4 \pm 0.4)\%$ ] accounts for the radiative tail in the  $E_\gamma$  distribution [Fig. 1(c)]. The photon-energy cut was varied from 8 to 36 GeV to test its effect on the value of  $r_\pi$ ; no significant effect was found. The tail of the  $\chi^2$  distribution [Fig. 1(b)] arises from radiative, track reconstruction, scattering, decay, and background effects. The  $\chi^2$  cut was varied from 10 to 80 with negligible effect on the pion radius. Corrections were made for radiative effects [ $(4.1 \pm 0.5)\%$  to  $(8.0 \pm 0.7)\%$ ], track reconstruction inefficiency [ $(2.7 \pm 0.5)\%$  to  $(3.3 \pm 0.8)\%$ ], primary pion attenuation [ $(3.3 \pm 0.1)\%$ ], secondary pion attenuation [ $(4.8 \pm 0.1)\%$ ], and geometric inefficiency [ $0.0\%$  to  $(27.0 \pm 2.3)\%$ ]. Analysis of events with low shower-counter pulse height [Fig. 1(d)] yielded a hadronic-interaction background correction of less than 1%.

The numbers of events which survive the cuts are listed in Table I as a function of  $q^2$ . Also given are the corrected numbers of events and the resulting cross section and square of the form factor. The square of the form factor is plotted in Fig. 2(a). The solid curve is a fit by a pole form  $|F_\pi|^2 = [1 - (r_\pi^2/6)q^2]^{-2}$  constrained to be unity at  $q^2=0$ . The error matrix is well represented by the statistical error and an overall normalization error of 1.0%. The  $\chi^2$  probability of the

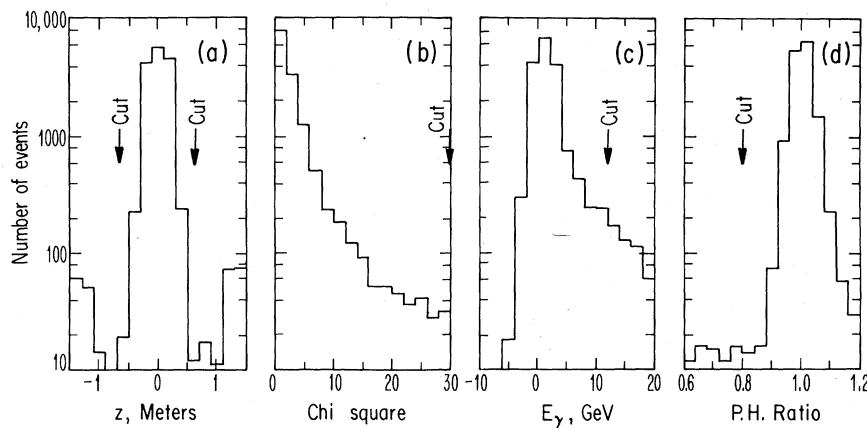


FIG. 1. Distributions of (a) reconstructed vertex position  $Z$ , (b)  $\chi^2$  for three-constraint fit, (c) fitted energy of radiated or bremsstrahlung photon, and (d) ratio of pulse height from the lead-glass shower counter to that expected, showing the cuts used in selecting elastic events.

TABLE I. Events (corrected in parentheses), measured cross section, and form factor vs  $q^2$ .

$q^2$ [(GeV/c) <sup>2</sup> ]	Number of events	$d\sigma/dq^2$ [ $\mu\text{b (GeV/c)}^{-2}$ ]	$ F_\pi ^2$
0.039	2583 (3895)	$123.9 \pm 2.7$	$0.857 \pm 0.019$
0.043	2184 (3150)	$100.3 \pm 2.4$	$0.865 \pm 0.021$
0.047	1738 (2440)	$77.6 \pm 2.0$	$0.821 \pm 0.022$
0.051	1496 (2069)	$65.8 \pm 1.8$	$0.840 \pm 0.024$
0.055	1238 (1716)	$54.6 \pm 1.6$	$0.831 \pm 0.025$
0.059	953 (1342)	$42.7 \pm 1.5$	$0.767 \pm 0.027$
0.063	873 (1255)	$39.9 \pm 1.4$	$0.838 \pm 0.029$
0.067	658 (978)	$31.0 \pm 1.3$	$0.757 \pm 0.032$
0.072	569 (886)	$28.1 \pm 1.2$	$0.791 \pm 0.035$
0.076	454 (747)	$23.6 \pm 1.2$	$0.762 \pm 0.038$
0.080	383 (662)	$20.9 \pm 1.1$	$0.765 \pm 0.041$
0.084	328 (607)	$19.3 \pm 1.1$	$0.802 \pm 0.045$
0.088	256 (483)	$15.3 \pm 1.0$	$0.720 \pm 0.047$
0.092	232 (432)	$13.7 \pm 0.9$	$0.728 \pm 0.050$

fit is 71% (14 data points with 13 degrees of freedom). The fitted mean square pion radius is  $r_\pi^2 = 0.439 \pm 0.30 \text{ fm}^2$ . A loose measure of internal consistency is provided by an unnormalized fit shown as the dashed line with  $r_\pi^2 = 0.384 \pm 0.088 \text{ fm}^2$  and a fitted value for  $|F_\pi|^2$  at  $q^2 = 0$  of  $0.974 \pm 0.039$ . The  $\chi^2$  probability of the latter fit is 68%. If the dipole form is used for the normalized fit instead of the pole form for  $|F_\pi|^2$ , the mean square radius becomes  $0.426 \pm 0.028 \text{ fm}^2$  and the  $\chi^2$  probability 70%.

The present results (F2) can be combined with the two earlier elastic-scattering experiments (S, F1). Figure 2(b) shows the square of the form factor obtained in these three experiments. A fit by the pole form was made to the 56 data points utilizing the full error matrix from each experiment. The result is shown as the solid curve in Fig. 2(b) and corresponds to  $r_\pi^2 = 0.405 \pm 0.024 \text{ fm}^2$  with a  $\chi^2$  of 51.0 for 55 degrees of freedom. Detailed results are given in Table II for each individual experiment and for their combination. If the constraint of  $|F_\pi|^2 = 1$  at  $q^2 = 0$  is removed, the overall fit to the three experiments yields  $r_\pi^2 = 0.454 \pm 0.067 \text{ fm}^2$  with fitted value  $|F_\pi|^2 = 1.021 \pm 0.027$  at  $q^2 = 0$  and  $\chi^2$  probability 62%.

The  $\chi^2$  value is indicative of a very good overall fit to the three experiments as is evident in Fig. 2(b). However, the statistical fluctuations mask systematic differences which are seen in the separate results for the pion radius squared; the F1 result is 2.1 standard deviations below the joint fit whereas the Serpukov and F2 results are

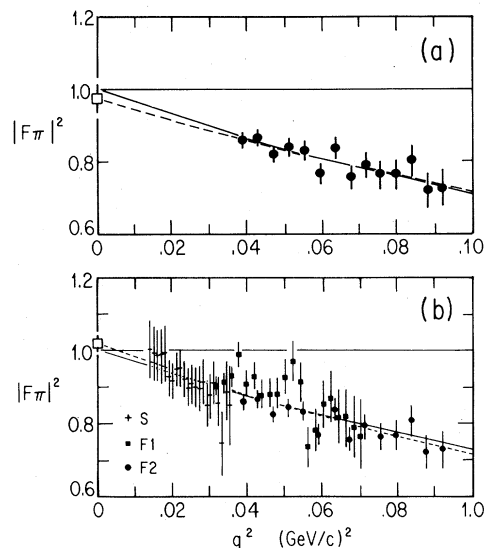


FIG. 2. Pion form factor squared vs  $q^2$  for (a) the present experiment (F2) and for (b) the experiments of Refs. 7 and 8 (S and F1) as well. The solid curves are fits with the constraint  $|F_\pi|^2 = 1$  at  $q^2 = 0$ . The dashed curves are unconstrained fits with fitted value at  $q^2 = 0$  indicated by the open-square points.

1.4 and 1.2 standard deviations above. This suggests that the experiments be combined with an error scale<sup>10</sup> of 2.0 and that the overall result with scaled error be taken as  $r_\pi^2 = 0.405 \pm 0.047 \text{ fm}^2$ .

Heyn and Lang<sup>11</sup> have done an analysis of pion form-factor data in the  $q^2$  region  $-9.61$  to  $+9.66 \text{ (GeV/c)}^2$  in a way which is largely model independent. They find  $r_\pi^2 = 0.47 \pm 0.02 \text{ fm}^2$ . If the electroproduction data of Bebek *et al.*<sup>6</sup> are excluded, they obtain  $r_\pi^2 = 0.43 \text{ fm}^2$  in good agreement with our present measurement (F2) of  $0.439 \pm 0.030 \text{ fm}^2$  and in fair agreement with the combined fit to all three direct measurement experiments (S + F1 + F2) of  $0.405 \pm 0.047 \text{ fm}^2$ .

The Chou-Yang model has been used to determine the pion radius from elastic pion-proton scattering.<sup>12</sup> The result depends upon the value of the proton's radius. With the proton radius determined by electron-proton scattering,  $r_\pi^2 = 0.30 \pm 0.01 \text{ fm}^2$ . With the proton radius determined by the Chou-Yang model itself applied to proton-proton scattering,  $r_\pi^2 = 0.44 \pm 0.01 \text{ fm}^2$ , in agreement with our direct determination from pion-electron elastic scattering (F2).

The negative-pion radius can be compared with those of other charged bosons. We measured the negative-kaon radius<sup>9</sup> with data taken simultane-

TABLE II. Results of fits of the pion form factor by the dipole form. Experiments S, F1, and F2 refer to Refs. 7, 8, and this experiment.

Experiment	Data points	$ F_{\pi^2} _{q^2=0} = 1$		$ F_{\pi^2} _{q^2=0} = \text{fitted quantity}$		
		$\langle r^2 \rangle, F^2$	$\chi^2$	$\langle r^2 \rangle, F^2$	Fitted normalization	$\chi^2$
S	22	$0.610 \pm 0.150$	9.6	$1.024 \pm 0.348$	$1.106 \pm 0.080$	7.7
F1	20	$0.315 \pm 0.041$	23.5	$0.418 \pm 0.145$	$1.039 \pm 0.052$	22.9
F2	14	$0.439 \pm 0.030$	9.8	$0.384 \pm 0.088$	$0.974 \pm 0.039$	9.3
S + F1 + F2	56	$0.405 \pm 0.024$	51.0	$0.454 \pm 0.067$	$1.021 \pm 0.027$	50.3

ously with the pion data reported here. The difference in mean square radius is  $r_{\pi^2} - r_K^2 = 0.16 \pm 0.06 \text{ fm}^2$  and is largely free from systematic errors. We are unaware of any reliable prediction for this result.

In summary, our new measurement of the negative-pion radius gives  $r_{\pi^2} = 0.439 \pm 0.030 \text{ fm}^2$  or  $r_{\pi} = 0.663 \pm 0.023 \text{ fm}$ , smaller than the proton but larger than the kaon by 2.7 standard deviations. Comparisons with previous elastic-scattering results<sup>7,8</sup> suggest an overall average of  $r_{\pi^2} = 0.405 \pm 0.047 \text{ fm}^2$  or  $r_{\pi} = 0.636 \pm 0.037 \text{ fm}$ , where the error has been enlarged to account for dispersion of the results. We find fair agreement with a global treatment of pion form-factor experiments particularly if electroproduction results are omitted. We also find good agreement with the Chou-Yang model provided that the Chou-Yang proton radius is used in the calculation. Finally, we await a fundamental theoretical calculation of the negative-pion radius.

We wish to thank Professor R. R. Wilson for his support and the many members of the Fermilab staff who assisted in bringing about this experiment. The work has been supported in part by the U. S. Department of Energy and in part by the National Science Foundation.

<sup>(a)</sup>Present address: Siemens Medical Laboratories,

Walnut Creek, Cal. 94596.

<sup>(b)</sup>Present address: Lawrence Berkeley Laboratory, University of California, Berkeley, Cal. 94720.

<sup>(c)</sup>Present address: Rutgers University, Piscataway, N. J. 08854.

<sup>(d)</sup>Present address: Hughes Aircraft Co., Culver City, Cal. 90230.

<sup>(e)</sup>Present address: High Energy Physics Laboratory, Stanford University, Stanford, Cal. 94305.

<sup>(f)</sup>Present address: Intersonics, Inc., Northbrook, Ill. 60062.

<sup>(g)</sup>Present address: Ohio State University, Columbus, Ohio 43210.

<sup>(h)</sup>Present address: Fermi National Accelerator Laboratory, Batavia, Ill. 60510.

<sup>1</sup>R. Hofstadter, Rev. Mod. Phys. **28**, 214 (1956).

<sup>2</sup>R. Wilson, in *Proceedings of the 1971 International Symposium on Electron and Photon Interactions at High Energy* (Cornell Univ. Press, Ithaca, 1972), pp. 97-114.

<sup>3</sup>We will use  $r$  for  $\langle r^2 \rangle^{1/2}$  and  $r^2$  for  $\langle r^2 \rangle$ .

<sup>4</sup>G. J. Gounaris and J. J. Sakurai, Phys. Rev. Lett. **21**, 244 (1968).

<sup>5</sup>A. Quenzer *et al.*, Phys. Lett. **76B**, 512 (1978).

<sup>6</sup>C. J. Bebek *et al.*, Phys. Rev. D **17**, 1693 (1978).

<sup>7</sup>G. T. Adylov *et al.*, Phys. Lett. **51B**, 402 (1974), and Nucl. Phys. B **128**, 461 (1977).

<sup>8</sup>E. B. Dally *et al.*, Phys. Rev. Lett. **39**, 1176 (1977), and Phys. Rev. D **24**, 1718 (1981).

<sup>9</sup>E. B. Dally *et al.*, Phys. Rev. Lett. **45**, 232 (1980).

<sup>10</sup>We have taken the error scale to be  $[\chi^2/(n-1)]^{1/2}$  as defined in Rev. Mod. Phys. **52**, 513 (1980).

<sup>11</sup>M. F. Heyn and C. B. Lang, Z. Phys. **7**, 169 (1981).

<sup>12</sup>T. T. Chou, Phys. Rev. D **19**, 3327 (1979).